ISTITUTO NAZIONALE DI FISICA NUCLEARE
Laboratori Nazionali di Frascati

LNF-83/107

S.Tazzari: FEL ACTIVITY IN FRASCATI INFN NATIONAL LABORATORIES

Estratto da:

"Free Electron Lasers", ed. by S.Martellucci and A.N.Chester (Plenum, 1983), p. 481

Servizio Documentazione
dei Laboratori Nazionali di Frascati
Cas. Postale 13 - Frascati (Roma)

From: FREE ELECTRON LASERS
Edited by S. Martellucci and Arthur N. Chester
(Plenum Publishing Corporation, 1983)

FEL ACTIVITY IN FRASCATI INFN NATIONAL LABORATORIES

S. Tazzari

I.N.F.N. - Laboratori Nazionali di Frascati
C.P. 13 - 00044 Frascati, Italy

1. INTRODUCTION

The Frascati National Laboratory (LNF) is operating a 1.5 GeV electron storage ring, Adone. The ring, designed and operated until 1978 mainly for high energy physics colliding beam experiments, is now dedicated to nuclear physics[1] and synchrotron radiation[2] research. A wiggler, designed to provide a hard X-ray beam,[3] is installed and operational. Although it has only three full periods, it can be operated in the undulator mode, to provide spontaneous radiation at visible wavelengths.

I am reporting on the work in progress on free electron lasers, which has developed along two lines: the study of the spontaneous radiation emitted by the existing undulator (wiggler) magnet, and the study of a FEL recirculated beam experiment to be performed on the storage ring.

The first measurements on the wiggler "coherent" beam have been performed[4] in the framework of a collaboration between LNF, the University of Naples, and the University of Trento.* They are discussed in Section 2.

*LNF: R. Barbini, M. Bassetti, M. E. Biagini, R. Boni, M.T. Capria, A. Cattoni, V. Chimenti, S. Guiducci, A. Luccio, M. Preger, C. Sanelli, M. Serio, S. Tazzari, F. Tazzioli, G. Vignola. Naples: E. Burattini, N. Cavallo, M. Foresti, C. Mencuccini, E. Pancini, P. Patteri, R. Rinzivillo, U. Troya. Trento: G. Dalba, F. Ferrari, P. Fornasini.

The FEL experiment, originally proposed[5] by R. Barbini* and G. Vignola*, has been approved by INFN early in 1980 and funded. It will be carried out in collaboration by LNF and the Universities of Naples and Bari. The outlines of the proposal are discussed in Section 3.

2. STUDY OF THE SPONTANEOUS RADIATION FROM THE WIGGLER MAGNET

2.1 Undulator Theory

We summarize the main features of undulator radiation:

a) For each observation angle θ, the radiation is composed of harmonics centered at

$$\lambda_h = \frac{\lambda_q}{2h\gamma^2}\,(1+K^2+(\gamma\theta)^2) \quad (h=1,2,3,\ldots) \tag{1}$$

where $\gamma = E/m_oc^2$ is the electron energy in unit of rest mass, K the undulator parameter and λ_q its wavelength.

b) The width of spectral peaks in the forward direction ($\theta = 0$) is

$$\frac{\Delta\lambda}{\lambda_h} \sim \frac{1}{hN} \tag{2}$$

where N is the number of undulator periods. For $\theta \neq 0$, there also appears an inhomogeneous broadening given by

$$\frac{\Delta\lambda}{\lambda_h} \sim \frac{\gamma^2\theta^2}{1+K^2} \tag{3}$$

c) The above line structure extends beyond $\theta_o = 1/\gamma$.

2.2 Spectrum Measurements in the Forward Direction: Preliminary Results

The main parameters of the Adone wiggler magnet[6,7] are listed in Table I.

By operating the magnet at very low current (51 A, corresponding to $B \simeq 200$ Gauss) a K of ~ 1, characteristic of the undulator regime, can be obtained.

*On leave from CNEN, Centro di Frascati.

With storage ring energies in the range from 500 to 800 MeV spontaneous coherent emission over the visible wavelength range is observed.

The experimental set-up to study the spectral characteristics of radiation emitted in the forward direction is schematically shown in Fig. 1.

The background radiation originating in the bending magnets next to the straight section where the wiggler is installed can be measured when the wiggler magnet is not energized, and subtracted out. Since the λ dependence of the background is known, the efficiency of the detector photomultiplier can also be taken care of.

Experimental results at γ = 1361.5 and γ = 1166.8 are shown in Fig. 2.

Table I. Wiggler Magnet

No. of poles	5 full + 2 half-poles
Gap height	40 mm
Total length	2100 mm
Pole-to-pole distance ($\lambda_q/2$)	327 mm
Maximum field	1.85 T
Max amperturns per pole	31,500
Max current	4500 A
Max power consumption	189 KW

The peak wavelength and intensity ratios are in agreement with the computation if K = 1.1, entirely consistent with the expected error on the estimate of K, is assumed.

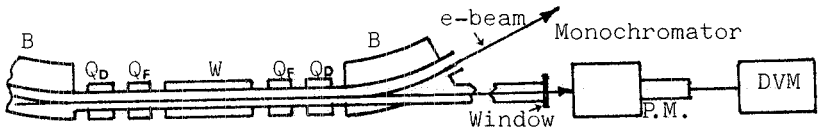

B, Q_D, Q_F are the bending magnets and quadrupoles of the ring;
W is the wiggler magnet.

Fig. 1. Schematic layout of experiment.

The shape and width of the measured distributions (∿ 40% f.w.h.h.) are not in agreement with the computation (∿ 30% f.w.h.h.). Possible causes for the discrepancy are being investigated, but it should be recalled that rather large systematic errors may be present in the subtraction procedure.

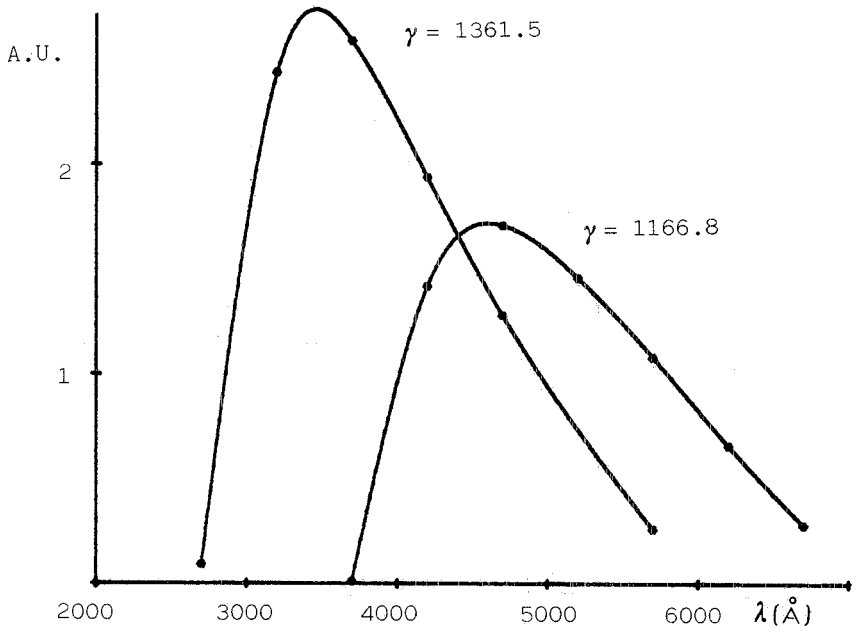

Fig. 2. Measured spectral distribution (first harmonic, $\theta = 0$) versus wavelength after background subtraction. The angular and wavelength resolutions are $\Delta\theta \simeq .1$ mr and $\Delta\lambda \simeq 380$ Å respectively.

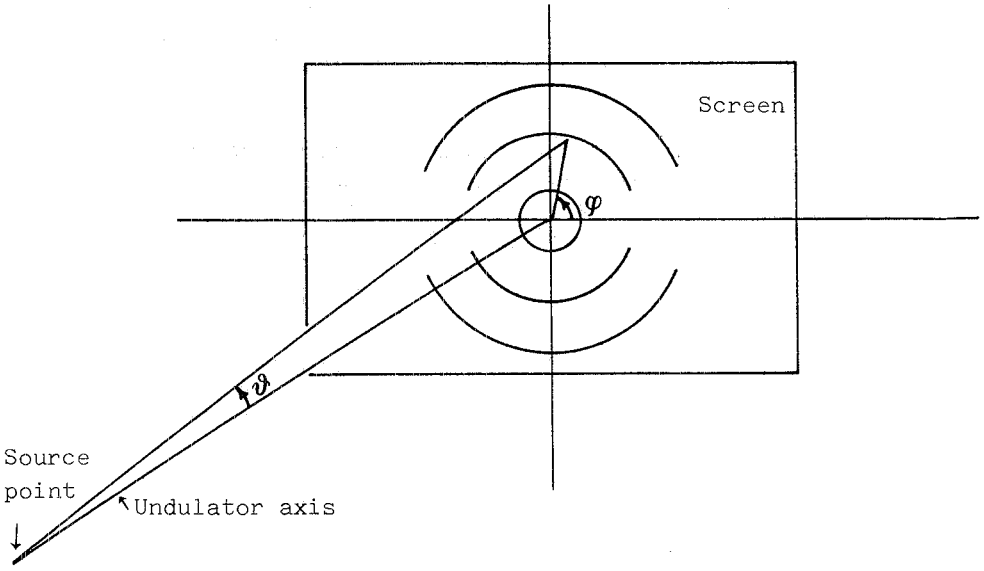

Fig. 3. Sketch of radiation pattern as observed on a screen.

2.3 Angular Distribution Measurements: Preliminary Results

The characteristic colored ring appearance of the undulator radiation as observed on a screen normal to the wiggler axis is schematically shown in Fig. 3. The dependence of peak wavelength λ on θ and on the harmonic number is shown in Fig. 4.

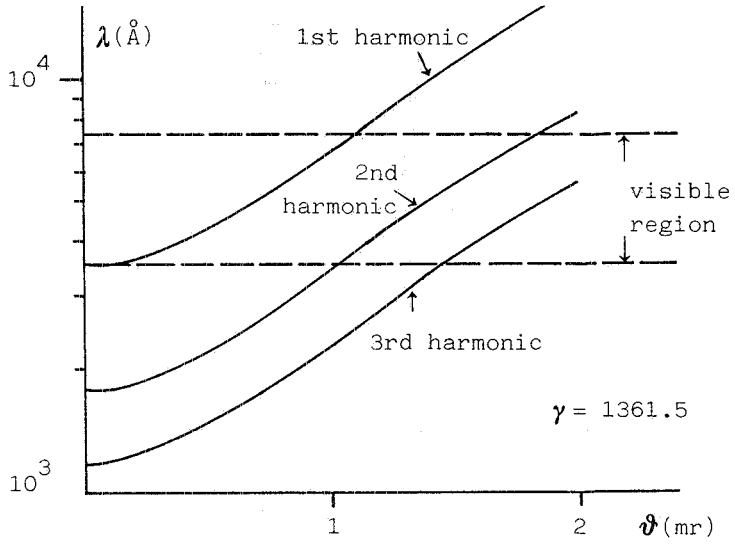

Fig. 4. Peak wavelength vs. θ.

In a number of patterns observed on a screen 14 meters away from the center point of the wiggler, at several machine energies in the range .5 to .8 GeV, harmonics up to the third were clearly visible.

Figures 5 and 6 show the intensity distribution of the central wavelength, as obtained from a computer code[8], as a function of θ and of the harmonic number, for $\psi = 0$ and $\psi = \pi/2$ respectively. The visible portions of the spectrum are indicated by a heavy line.

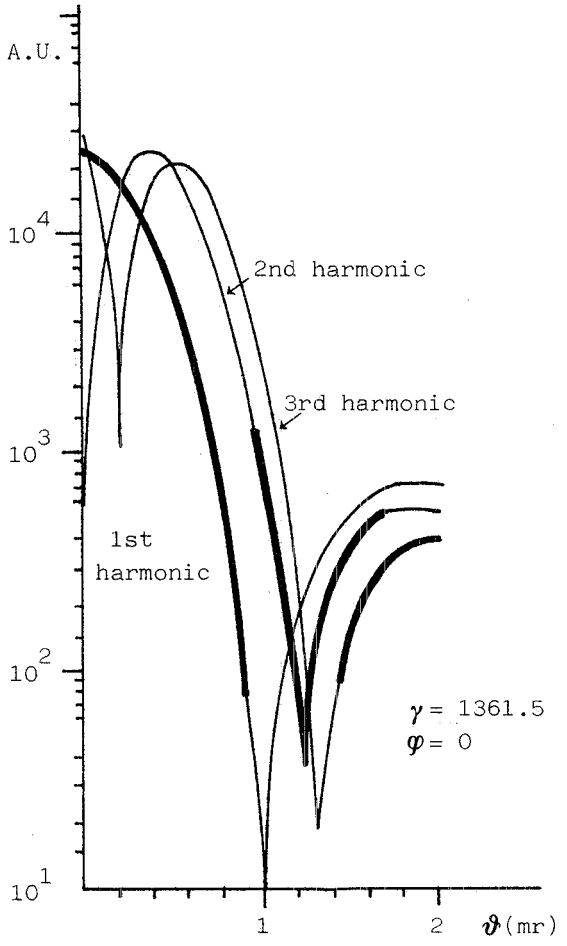

Fig. 5. Intensity distribtuion of peak wavelength vs. θ for $\psi = 0$.

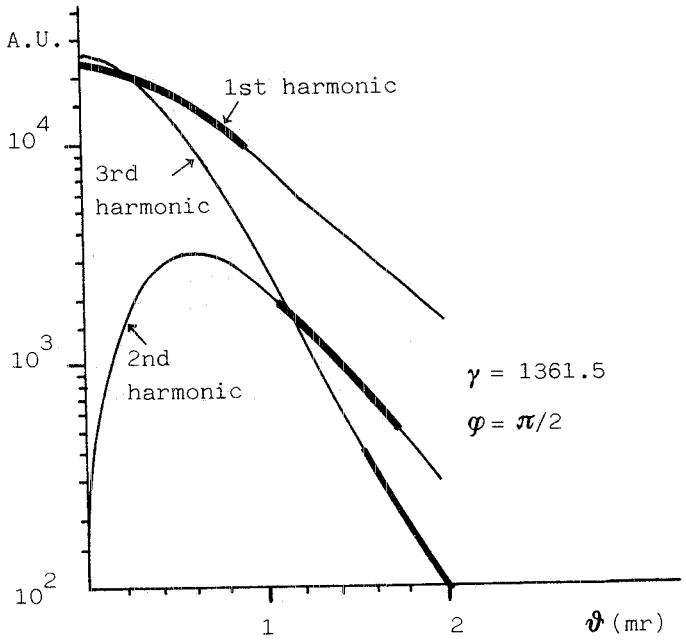

Fig. 6. Intensity distribution of peak wavelength vs. θ for $\psi = \pi/2$.

The computed distributions seem to explain very well the observed patterns; in particular the expected intensity drops at around $\psi = 0$ clearly appear as dark spots at the correct values of θ.

More precise measurements are needed, including a densitometric analysis to check that intensities are in the predicted ratios.

3. THE DESIGN OF A FREE ELECTRON LASER EXPERIMENT ON ADONE (LELA)

3.1 Goals

The main goal of the LELA experiment[5] is to collect information on the following topics:

- amplification of radiation with the aid of an external "seed" laser (Argon laser λ = 5145 Å);
- wavelength and optical gain as functions of electron energy and undulator magnetic field;
- transient behavior of the laser radiation;
- steady-state interaction between laser radiation and stored electrons (i.e., optical gain vs. electron energy, maximum optical output power, optical spectrum).

3.2 FEL and Storage Ring Parameters

It is proposed to install a transverse undulator on one of the Adone straight sections. An external laser beam can be sent along the straight section axis to interact with the electron beam and the undulator field (see Fig. 11), or an optical cavity can be built by adding a mirror at each end of the straight section.

In order to minimize the laser beam losses in the optical cavity (oscillator experiment) and to avoid head-on collisions between photons and electrons, it is convenient to operate Adone with three electron bunches and to adjust the optical cavity length to half the distance between two consecutive bunches: a single photon bunch will then travel inside the optical cavity and will meet one of the electron bunches once every round trip.

The spontaneous radiation wavelength observed on the undulator axis is given by (1) (with $\theta = 0$, $h = 1$), and can be tuned by varying either the electron energy or the undulator magnetic field or both.

The undulator parameters are listed in Table II.

For a pure cosine-like vertical magnetic field

$$B_z = B_o \cos \frac{2\pi}{\lambda_q} y \tag{4}$$

the parameter K is given by

$$K = \frac{eB_o \lambda_q}{\sqrt{2}\, 2\pi m_o c} \simeq 6.6\, B_o\ (KG)\ \lambda_q(m). \tag{5}$$

By defining the R.M.S. magnetic field on axis by

$$\overline{B} = \left[\frac{1}{\lambda_q} \int_o^{\lambda_q} |B_z(y)|^2\, dy \right]^{1/2} \tag{6}$$

one can also write

$$K = 9.33\, \overline{B}\ (KG)\ \lambda_q(m). \tag{7}$$

In order to avoid all unnecessary technical complications, it is best to operate in the visible wavelength region with magnetic fields that can be achieved by standard magnet technology. The electron energy should be the highest possible in order to achieve the highest possible peak current (see § 3.3). The undulator period should be designed so as to accomodate the maximum number of periods

in the fixed length of the Adone straight section (2.5 m). On the other hand, the achievable magnetic field on axis will depend both on the undulator period and on the gap height.[9,10] Finally, electron energy, undulator period and magnetic field are connected by the wavelength equation (1).

Taking into account the above constraints and using the results of magnetic field calculations[11] one ends up with the basic FEL parameters listed in Table II.

The FEL gain has been demonstrated[12] to be inversely proportional to the square of the total spontaneous radiation linewidth, which, in turn, is made up of two contributions, homogeneous and inhomogeneous broadening, adding quadratically. The inhomogeneous broadening is usually required to be negligible with respect to the homogeneous one.

Table II. FEL Parameters

Undulator period	$\lambda_q = 11.6$ cm
Number of periods	$N = 20$
Undulator length	$L_w = 2.32$ m
Homogeneous broadening	$\left[(\Delta\lambda/\lambda)\right]_o = \lambda_q/2L_w = 2.5\%$
RMS magnetic field on axis	$\overline{B} = 3153$ G $K = 3.412$
Electron energy	$E = 610$ MeV
Radiation wavelength	$\lambda = 5145$ Å
Optical cavity length	$L = 17.5$ m

This places upper limits on the e-beam angular divergence and energy spread. It also requires the off energy η function to vanish at the place where the undulator is mounted.

By increasing the number of independent quadrupole families from 2 to 4, Adone can be made into a six-period machine with η vanishing in alternative straights, thus satisfying the requirements. The standard cell and the resulting functions are shown in Fig. 7. The main machine parameters for this new structure are listed in Table III. In the table, it has been assumed that a new 51.4 MHz RF cavity, at present under test, will be installed and operating (see also § 3.3).

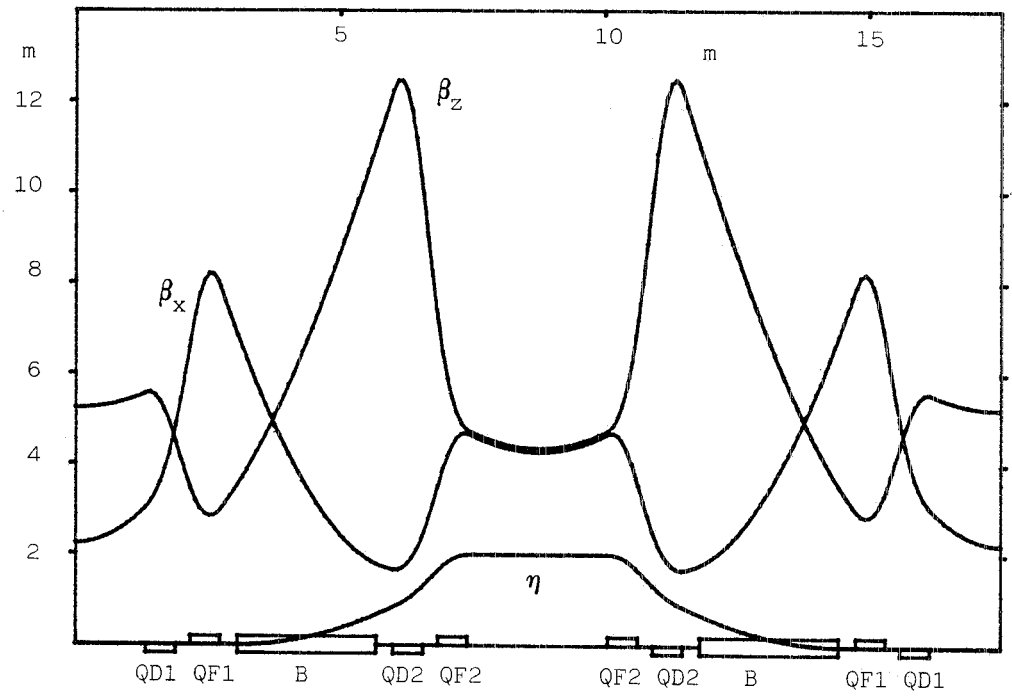

Fig. 7. Optical functions for the standard cell.

3.3 Small Signal Gain

The FEL small signal gain per pass in the homogeneous broadening regime and for a monochromatic e-beam is:[13]

$$g_o = -32\sqrt{2}\,\pi^2\lambda^{3/2}\,\lambda_q^{1/2}\,\frac{K^2}{(1+K^2)^{3/2}}\,\frac{I_p}{I_A}\,\frac{N^3}{\Sigma_L}\,f(x) \qquad (8)$$

where

$I_A = \frac{ec}{r_o} = 17.000$ A, $\quad \gamma_o$ = operating energy (in unit of $m_o c^2$),

I_p = peak current/bunch, $\quad \gamma_R$ = resonance energy $= \left[\frac{\lambda_q}{2\lambda}(1+K^2)\right]^{1/2}$,

$x = 4\pi N \frac{\gamma_o - \gamma_R}{\gamma_R}$, $\quad f(x) = -\frac{1}{x^3}\left\{\cos x - 1 + \frac{1}{2}x \sin x\right\}$.

The function f(x) is plotted in Fig. 8 and is proportional to the derivative of the spontaneous emission lineshape

$$\left(\frac{\sin x/2}{x/2}\right)^2.$$

By assuming it has its maximum value (= -0.0675 for x = 2.6056) and taking for the E.M. beam cross section the value $\overline{\Sigma}_L = L_w\lambda/\sqrt{3}$ (see § 3.5), with the parameters listed in Table II the gain g_o can be written

$$g_o = 6.7 \times 10^{-4} I_p(A) \simeq 3 \times 10^{-3} \frac{i(mA)}{\sigma_y(cm)} \qquad (9)$$

$I_p(A)$ is the peak current/bunch, i(mA)is the mean current/bunch, and σ_y is the R.M.S. bunch length.

Table III. Machine Parameters

Electron energy	E = 610 MeV
Momentum compaction	$\alpha_c = 1.36 \times 10^{-2}$
Fractional energy spread	$\sigma_p = 2.3 \times 10^{-4}$
Invariant	<H> = 0.38 m
Radial emittance (off coupling)	A_x = 0.25 mm x mrad
Energy loss in bending magnets	U_o = 2.45 KeV/turn
Energy loss in undulator	U_w = 109 eV/pass
Radial betatron tune	ν_x = 5.15
Vertical betatron tune	ν_z = 3.15
Radial natural chromaticity	C_x = -1.06
Vertical natural chromaticity	C_z = -1.61
Damping partition numbers	$J_s = 2$; $J_x = J_z = 1$
Damping times	$\tau_i = 184/J_i$ msec
Revolution frequency	f_o = 2.856 MHz
RF frequency	f_{RF} = 51.4 MHz
Harmonic number	h = 18
Number of bunches	n_b = 3
1 RF cavity: RF peak voltage	V_{RF} = 300 KV
RF acceptance	ε_{RF} = 3.58%
2 RF cavities: RF peak voltage	V_{RF} = 600 KV
RF acceptance	ε_{RF} = 5.06%

The optical gain per pass must exceed the cavity losses: the computed diffraction losses are negligible, and it is assumed that mirror absorption and transmissivity can reasonably be kept below 4% total. The gain is therefore required to be at least of the order of a percent. This value can be obtained with mean currents of some tens of mA/bunch and σ_y's of the order of a few cm. At 610 MeV the anomalous bunch lengthening phenomenon must however be properly taken into account.

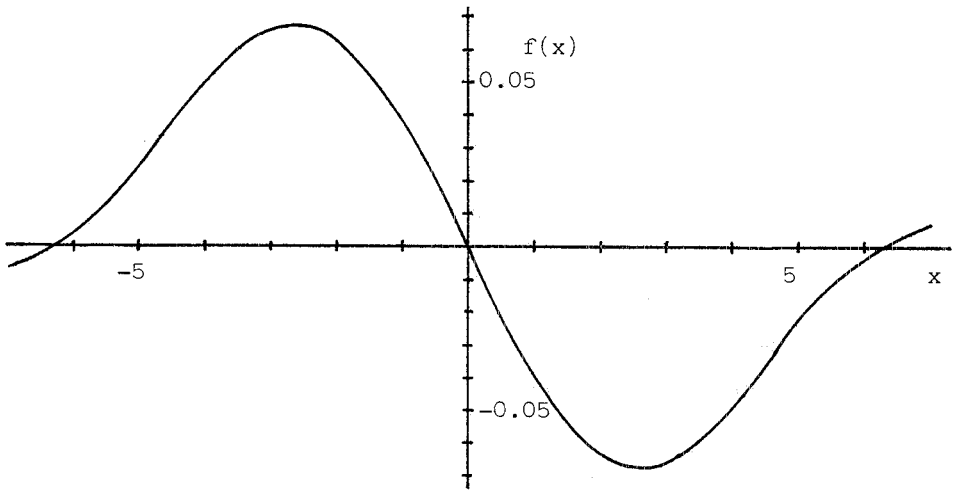

Fig. 8. The gain function.

3.4 Bunch Lengthening

By extrapolating the results on bunch lengthening obtained for Adone to the new structure, using a Chao-Gareyte[14] model, σ_y can be written as

$$\sigma_y \text{ (cm)} \simeq 29 \left[\frac{i(\text{mA})}{V_{RF}(\text{KF})}\right]^{.37} \tag{10}$$

By inserting eq. (10) into (9) one obtains:

$$g_o \simeq 10^{-4}\, i_{(\text{mA})}^{.63} \times V_{RF(\text{KV})}^{.37} \tag{11}$$

In Fig. 9, the R.M.S. bunch length σ_y is plotted vs. bunch current both with and without anomalous lengthening, and for the two cases V_{RF} = 300 KV and V_{RF} = 600 KV. Figures 10a and 10b show the corresponding gain curves.

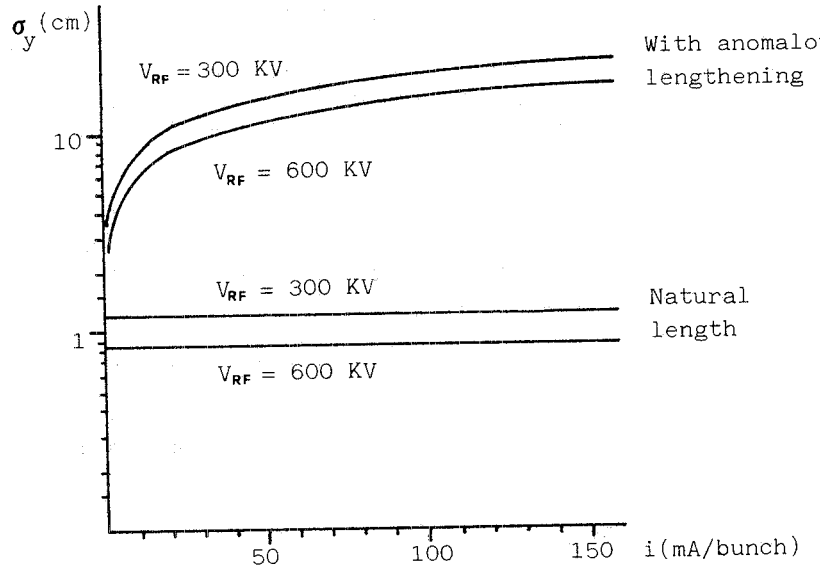

Fig. 9. Natural and anomalous bunch length σ_y of V_{RF} = 300 KV and V_{RF} = 600 KV.

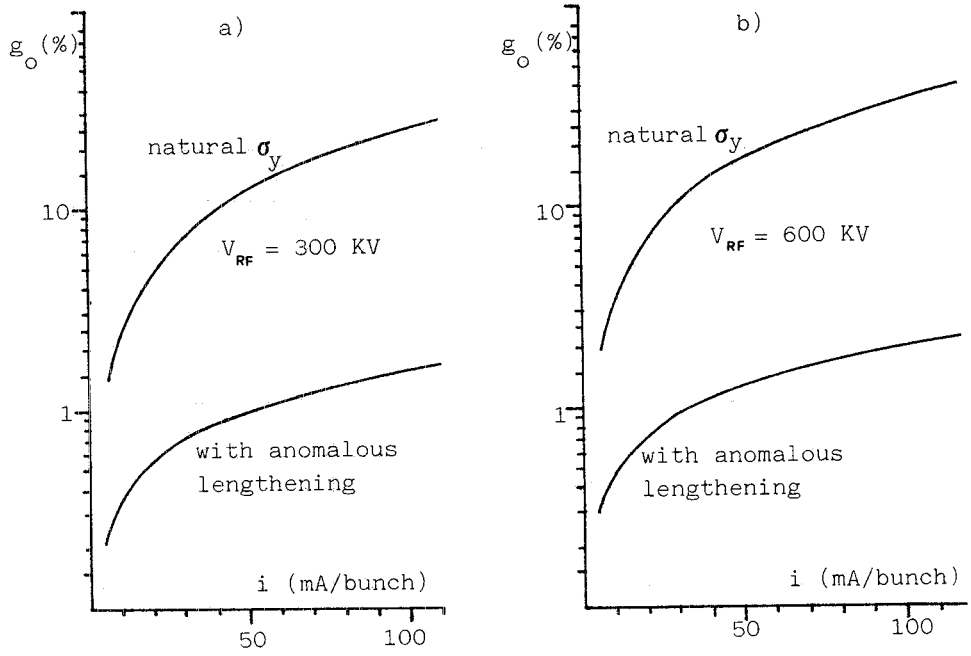

Fig. 10. Optical gain/pass vs. mean current bunch.
a) V_{RF} = 300 KV. b) V_{RF} = 600 KV.

We conclude that the anomalous lengthening significantly affects the gain. Accurate measurements at the energy and currents considered, with the new RF system, will have to be performed. It is at present felt that the Chao-Gareyte type extrapolation gives an upper limit to the anomalous lengthening and, consequently, a lower limit to the gain.

3.4 Electron Beam Lifetimes

In evaluating electron beam lifetimes, the contributions from single and multiple Touschek effects, vacuum chamber aperture and RF acceptance, have to be considered.

Lifetimes are calculated assuming a gaussian e-beam distribution. Actually, in a steady state laser operation, electrons should have a harmonic oscillator energy distribution whose tails are steeper than those of a gaussian. This could lead to lifetimes longer than those computed in the following sections.

3.4.1 Touschek Effect

A computer code developed by F. H. Wang[15] shows that, for i = 50 mA/bunch, the Touschek lifetimes τ_T (including multiple Coulomb scattering) and the beam cross section enlargement ratios ζ are those listed in Table IV (see also ref. 16).

Table IV. Touschek Lifetimes

	V_{RF} = 300 KV		V_{RF} = 600 KV	
	τ_T (hours)	ζ	τ_T (hours)	ζ
Without anomalous lengthening	22.9	2.05	48.2	2.24
With anomalous lengthening	449	1.08	1056	1.10

3.4.2 Vacuum Chamber Aperture

We recall[17] that the total radial spread can be written as

$$\sigma_x^2 = \sigma_{x\beta}^2 + \sigma_{x\varepsilon}, \tag{12}$$

where

$$\sigma_{x\beta}^2 = \sigma_p^2 \langle H \rangle_{mag} \left(\frac{J_s}{J_x} \right) \beta_x \frac{1}{1 + \chi^2} \tag{13}$$

is the betatron contribution (χ^2 is the coupling coefficient for betatron oscillations) and $\sigma_{x\varepsilon}^2$ is the energy spread contribution.

Without making any assumption on the transient behavior, it can reasonably be assumed that if a steady state is to be reached, the R.M.S. electron energy spread will reach the equilibrium value[18]

$$\frac{2\Delta\gamma}{\gamma} = \frac{1}{2N}, \tag{14}$$

so that

$$\sigma_{x\varepsilon} \approx \frac{\Delta\gamma}{\gamma} \approx \eta \frac{1}{4N} \tag{15}$$

This will soon become the dominant contribution to the total spread (12) where $\eta \neq 0$.

At equilibrium, the beam lifetime is[16]

$$\tau_{qx} = \tau_x \, e^{(d/\sigma_{x\varepsilon})^2} \left(\frac{\sigma_{x\varepsilon}}{d} \right)^2 \tag{16}$$

where d is the half width of the vacuum chamber. With d = 7 cm, τ_x = 174 msec and η = 2 m, we get:

$$\tau_{qx} \approx 56 \text{ sec.} \tag{17}$$

3.4.3 RF Acceptance

With similar arguments the beam lifetime for energy oscillations, assuming a gaussian energy spread distribution function, can be written:

$$\tau_q = \tau_s \, e^{(\varepsilon_{RF}/\frac{\Delta\gamma}{\gamma})^2} \left(\frac{\Delta\gamma/\gamma}{\varepsilon_{RF}} \right)^2 . \tag{18}$$

With τ_s = 87 msec one has

$$\tau_{q\varepsilon} \simeq 38 \text{ sec} \quad (1 \text{ RF cavity}), \tag{19}$$

$$\tau_{q\varepsilon} \simeq 19 \text{ hours} \quad (2 \text{ RF cavities}). \tag{20}$$

3.5 Optical Parameters

According to Eq. (8), the FEL gain is inversely proportional to the optical mode cross section $\bar{\Sigma}_L$ in the interaction region, provided the electron beam is fully contained with the laser beam ($\Sigma_e < \bar{\Sigma}_L$).

The laser beam cross section $\bar{\Sigma}_L$ is given by

$$\bar{\Sigma}_L = \frac{1}{L_w} \int_{-L_w/2}^{L_w/2} \Sigma(y)dy = \frac{2\pi w_o^2}{L_w} \int_0^{L_w/2} \left[1 + \left(\frac{\lambda y}{\pi w_o^2}\right)^2\right] dy \tag{21}$$

where L_w is the length of the interaction region and w_o is the beam waist for a TEM_{oo} gaussian mode.

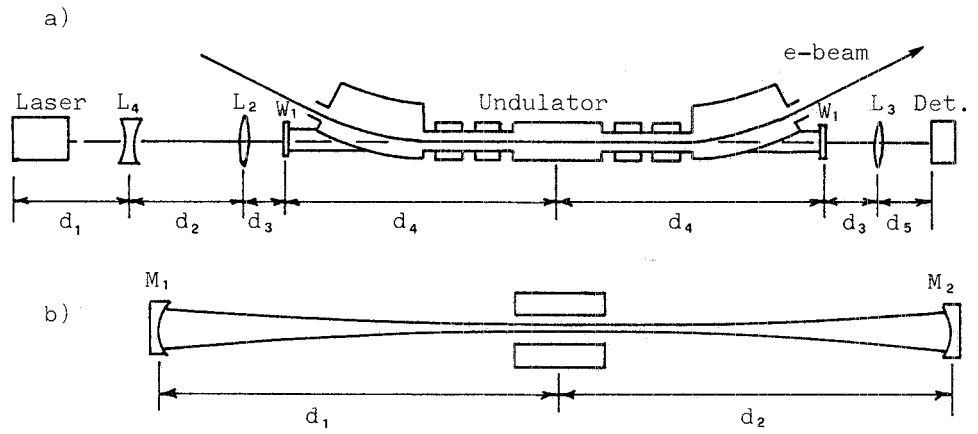

Fig. 11. a) Schematic layout of the amplification experiment.
b) Schematic layout of the oscillation experiment.

The optimum beam waist can be found by minimizing the mode cross section

$$\frac{d}{dw_o} \bar{\Sigma}_L = 0 \ , \tag{22}$$

which implies

$$w_o = \sqrt{\frac{L_w \lambda}{2\pi \sqrt{3}}} \ . \tag{23}$$

By substituting Eq. (23) into Eq. (21), we have:

$$\bar{\Sigma}_L = \frac{L_w \lambda}{\sqrt{3}} \ . \tag{24}$$

For $\lambda = 5145$ Å (our experiment) the optimum beam waist becomes $w_o \approx 0.35$ mm.

3.6 The Amplification Experiment

A possible layout of the amplification experiment is sketched in Fig. 11a. Here L_i are spherical lenses with focal lengths F_i and W_i are quartz windows. The "seed" laser to be used will be the Spectra-Physics SP 164-09 model operating in single line mode at 5145 Å. In order to have $w_o = 0.35$ mm at the undulator mid-point[17] distances and focal lengths can be chosen as follows:

$d_1 = 2.60$ m; $d_2 = 2.69$ m; $d_3 = 0.40$ m; $d_4 = 6.0$ m; $d_5 = 0.91$ m

$F_1 = -2.5$ m; $F_2 = 2.5$ m; $F_3 = 0.8$ m.

3.7 The Oscillator Experiment

The optical cavity parameters must also be chosen so as to produce a waist $w_o = 0.35$ mm at the center of the interaction region for a wavelength $\lambda = 5151$ Å.

In Fig. 11b, M_i are concave mirrors with curvature radii R_i.

Table V shows the computed optical cavity parameters. W_i are the beam sizes on the mirrors and the corresponding Fresnel numbers, $N = a^2/d\lambda$, are calculated assuming the mirror size, a, is equal to the largest w_i.

Fig. 12 shows the e-beam and laser beam profiles along the interaction region both in the radial and in the vertical plane.

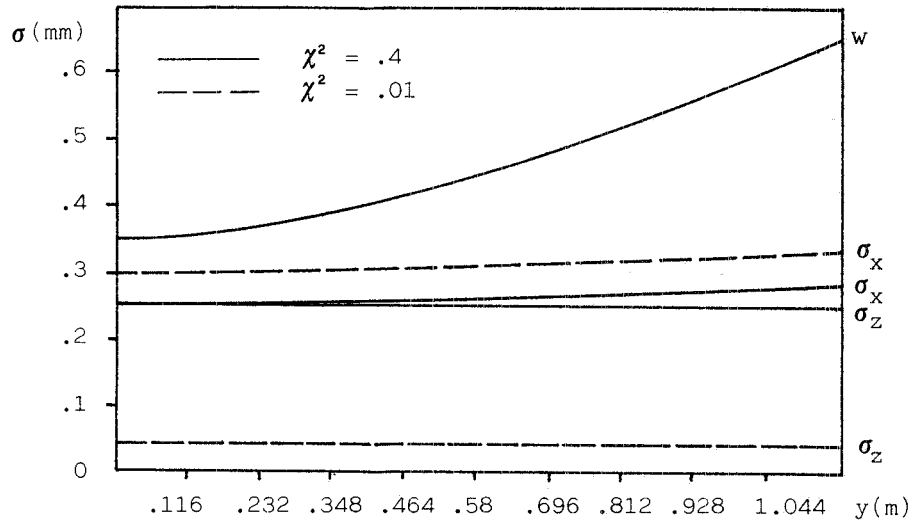

Fig. 12. Electron beam and laser beam profiles, along the interaction region.

Table V. Optical Cavity Parameters

d_1(m)	d_2(m)	w_o(mm)	w_1(mm)	w_2(mm)	R_1(m)	R_2(m)	$\mathcal{N}$	$\left(1-\frac{d_1+d_2}{R_1}\right)\left(1-\frac{d_1+d_2}{R_2}\right)$
8.75	8.75	0.35	4.14	4.14	8.81	8.81	2.2	0.973

The e-beam dimensions are plotted for two values of the betatron oscillation coupling factor $\chi^2 \approx 0.42$ (circular e-beam) and $\chi^2 \approx 0.01$, the latter corresponding to the minimum coupling so far obtained in Adone and gives a rather flat beam.

The detailed design of the optical cavity under vacuum is in progress.

3.8 Optical Klystron

The design of the proposed undulator makes it rather easy to change the coil interconnections in such a way as to produce an optical klystron type magnetic field configuration.[19]

Another possibility is to have two undulators in two adjacent straight sections, using the ring bending magnet in between as a dispersive drift space.

An optical klystron set-up, even with its inherently lower saturation output power, could become very interesting if the gain of the conventional FEL is found to be marginal.

Calculations for our case are in progress and some of the preliminary results have been presented during this school[20] by I. Boscolo.

Acknowledgements

The help from R. Barbini and G. Vignola in critically reading and in the editing of this paper, is gratefully acknowledged.

REFERENCES

1. R. Caloi et al.: A new monochromatic and polarized photon beam at Frascati. Proc. Intern. Conf. on Nuclear Physics with Electromagnetic Interactions, Mainz, 1979; LNF-79/30(P).
2. P.U.L.S. (CNR/GNSM-INFN): Rapporto di attivita 1977. LNF.
3. M. Bassetti, M. E. Biagnini, R. Boni, E. Burattini, M. T. Capria, A. Cattoni, N. Cavallo, V. Chimenti, G. Dalba, F. Ferrari, M. Foresti, P. Fornasini, S. Guiducci, A. Luccio, C. Mencuccini, E. Pancini, P. Patteri, M. Preger, R. Rinzivillo, C. Sanelli, M. Serio, S. Tazzari, F. Tazzioli, U. Troya: The Adone wiggler facility (to be published).
4. R. Barbini, E. Burattini, C. Cattoni, M. T. Capria, G. Vignola: Prime misure sulla radiazione coerente dal wiggler. Adone Int. Memo RM-22 (1/9/80).
5. R. Barbini, G. Vignola: LELA: A free electron laser experiment in Adone. Frascati Report LNF-80/12(R), March 1980.
6. M. Bassetti, A. Cattoni, A. Luccio, M. Preger and S. Tazzari: A. transverse wiggler magnet for Adone. Frascati Rep. LNF-77/26 ('77).
7. M. Bassetti, S. Tazzari in "Wiggler meeting," Frascati, June 29-30, 1978, ed. by A. Luccio, A. Reale and S. Stipcich (LNF, 1978).

8. R. Barbini and G. Vignola: The LELA undulator as a source of synchrotron radiation. Adone Internal Memor G-32 (1979).
R. Barbini, M. T. Capria, G. Vignola: Angular distribution of the Adone wiggler synchrotron radiation. Adone Internal Memo G-35 (1979).
9. Groupe "Supraconducteurs", CEN-Saclay Report DPh/Pe-STRIP SUPRA 78-35 (1978).
10. A. Cattoni: Progetto di massima di un ondulatore per il FEL; Adone Internal Memo MA-45 (1979).
A. Cattoni, C. Sanelli: Calcolo di un ondulatore per Adone: minimo λq. Adone Int. Memo MA-46 (1979).
B. Dulach: Ondulatore: calcolo delle deformazioni meccaniche. Adone Int. Memo M-7 (1979).
11. R. Barbini, M. E. Biagini and G. Vignola: Sul campo magnetico dell'on dulatore per il FEL. Adone Int. Memo MA-44 (1979).
12. L. R. Elias, W. M. Fairbank, J. M. J. Madely, H. A. Schwettman and T. I. Smith, Phys. Rev. Letters 36, 717 (1976).
D. A. G. Deacon, L. R. Elias, J. M. J. Madey, G. J. Ramian, H. A. Schewettman and T. I. Smith, Phys. Rev. Letter 38, 892 (1977).
W. B. Colson, Phys. Letters 59A, 187 (1976); 64A, 190 (1977).
13. C. Pellegrini, IEEE Trans. on Nuclear Sci., NS-26, 3791 (1979).
C. Pellegrini in "Report on FEL Workshop", Riva del Garda, June 4-6, 1979, ed. by G. Scoles.
14. A. W. Chao and J. Gareyte: Scaling law for bunch lengthening in SPEAR II, Report SPEAR 197/PEP 224 (1976).
S. Tazzari: Scaling dell'allungamento anomalo, Adone Int. Memo T-93 (1978).
15. F. H. Wang: Touschek lifetime at Adone and beam size. Adone Int. Memo T-113 (1979).
16. H. Bruck, Accelerateurs Circulaires de Particules (Presses Univ. de Feance, 1966).
17. M. Sands: The physics of electron storage rings. An introduction. Report SLAC-121, UC-28(ACC) (1970).
18. G. Dattoli, A. Renieri: Nuovo Cimento B, 59, 1 (1980).
19. N. A. Vinokuronov, A. N. Shrinsky, Proc. of the 6th National Conf. on Charged Particle Accelerators. Dubna, 1978, vol. 2.
A. S. Artamov, N. A. Vinokurov, P. D. Voblyi, E. S. Gluskin, G. A. Kornyukhin, V. A. Kochubei, G. N. Kulipanov, V. N. Litvinenko, N. A. Mezentsev and A. N. Skrinsky: The first experiments with an optical kylstron installed on the VEPP-3 storage ring. Novosibirsk Preprint, 1980.
20. I. Boscolo and V. Stagno: The coherent emission from a bunched electron beam in a wiggler. These Proceedings.